International Journal of Microwave and Wireless Technologies, 2012, 4(6), 629–634.
doi:10.1017/S1759078712000633

RESEARCH PAPER

Far-field formulation of a Cassegrain reflector using a novel illumination function and aperture field integration

MOHAMMAD ASIF ZAMAN AND MD. ABDUL MATIN

In this paper, the far-field pattern of a Cassegrain reflector is formulated. A novel illumination function is used to approximate the field distribution at the aperture of the reflector. The defined illumination function takes into account the central aperture blockage created by the subreflector. Using the illumination function, a closed-form expression describing the far-field radiation pattern of the Cassegrain reflector is formulated. The radiation pattern obtained from the derived equation is compared with the results obtained from physical optics and physical theory of diffraction. The results are found to be consistent with each other. It is found that the derived results show an impressive accuracy of 99.8% over the main-lobe region. The accuracy is found to be over 91 and 84% for the first and second significant side-lobe region, respectively, which can be considered satisfactory for many applications.

Keywords: Aperture blockage, Aperture field integration, Cassegrain reflector, Far-field, illumination function, Radiation pattern

Received 16 February 2012; Revised 22 August 2012; first published online 19 September 2012

I. INTRODUCTION

Cassegrain reflector antennas are widely used in satellite communication, radar applications, remote sensing, radio astronomy, etc. These antennas are characterized by their highly directive nature, and relatively large aperture efficiency. Demand for Cassegrain reflectors has resulted in the development of numeric and analytic techniques for design and analysis of such antennas [1, 2].

A Cassegrain antenna consists of a feed antenna, a hyperboloidal subreflector, and a paraboloidal main reflector. When the antenna is used as a transmitter, the electromagnetic radiation from the feed antenna, which is usually a horn antenna, is directed toward the subreflector. The subreflector is said to be illuminated by the feed antenna. The subreflector scatters the incident field and in doing so, illuminates the main reflector. The main reflector creates the far-field radiation pattern of the antenna. The far-field pattern from the main reflector is called the secondary pattern and the radiation pattern of the feed antenna is known as the primary pattern [3]. The secondary pattern depends on the geometry of the Cassegrain system, and the primary pattern [3, 4].

Several methods exist for formulating the far-field of a Cassegrain reflector. Geometrical optics (GO), uniform geometrical theory of diffraction (UTD), physical optics (PO), and physical theory of diffraction (PTD) are widely used numerical methods for large Cassegrain antennas [5]. These methods are sufficiently accurate, but they require lengthy calculations and tedious computer coding. In many cases, only the main lobe region near the bore-sight of the Cassegrain antenna needs to be calculated, as the far-off sidelobes have very small values [4]. Sufficiently accurate results for the near main lobe region can be obtained by using justified approximations. These approximation methods can provide a simpler alternative for estimating the far-field region near the bore-sight of the antenna.

The aperture field (AF) integration method provides an opportunity to use approximation techniques to derive closed-form expressions for the far-field region [5, 6]. In the AF integration method, the fields reflected by the main reflector are approximated by GO rays. The reflected rays from the main reflector are projected upon an infinite plane. This plane is called the aperture plane of the antenna [1, 4]. The aperture plane is usually assumed to go through the focus of the paraboloid. The observation point P is taken to be far away from the aperture plane. A Cassegrain antenna along with its aperture plane is shown in Fig 1. The projected field on the aperture plane is known as the AF of the antenna. The aperture of the antenna is defined as the projected surface of the main reflector on the aperture plane. The AF outside the aperture is approximated as zero [1]. The radiation integral over the curved surface of the main reflector can equivalently be performed over the aperture plane of the antenna. This method is known as the AF integration method.

By knowing the field distribution on the aperture of the antenna, the far-field pattern can be calculated using AF integration [6, 7]. The AF depends on the primary pattern and the

Department of Electrical and Electronic Engineering, Bangladesh University of Engineering and Technology, Dhaka 1000, Bangladesh. Phone: +8801712646464
Corresponding author:
M. Asif Zaman
Email: asifzaman13@gmail.com; zaman@eee.buet.ac.bd

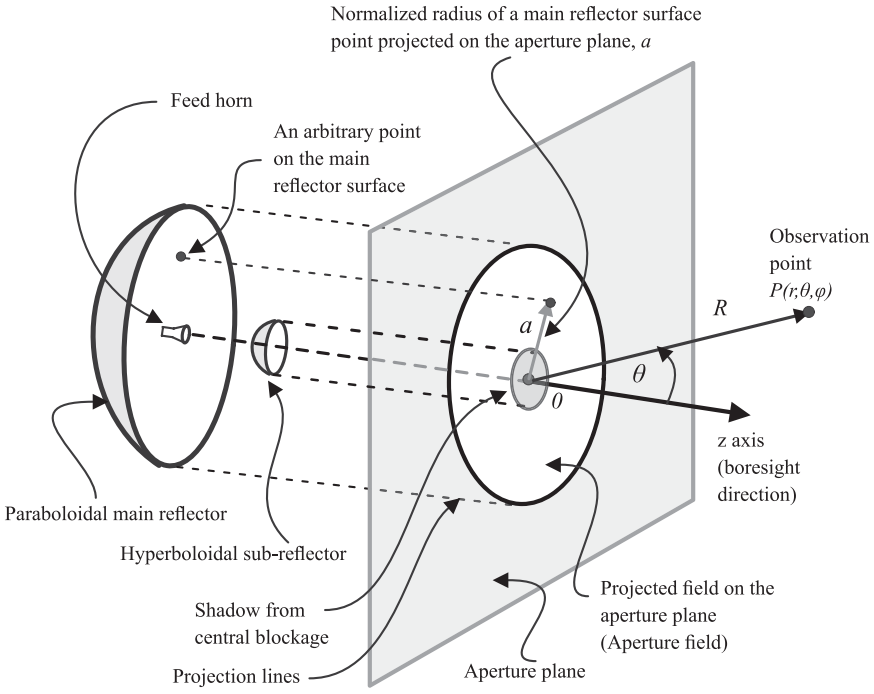

Fig. 1. Apeture plane of a Cassegrain antenna.

subreflector surface geometry. In an unshaped Cassegrain system, the subreflector is a hyperboloid. In such cases, only the primary pattern determines the AF. In most cases, the feed antenna is a horn antenna, such as a conical corrugated horn or a potter horn [1]. The AF resulting from these types of feeds can be modeled by mathematical functions containing a few parameters. These functions are known as illumination functions [8, 9]. The accuracy of the AF integration depends on how well the illumination function represents the actual AF distribution.

It can be seen from Fig 1 that a part of the aperture of the antenna is shadowed by the subreflector. This is known as the central aperture blockage. Owing to the aperture blockage, the AF in the shadowed region has smaller value. This reduction in AF value causes the overall gain of the antenna to decrease [4, 10]. Aperture blockage may also be created by subreflector supports [11]. However, compared with the subreflector blockage, these blockages are negligible. To correctly approximate the AF, the illumination function must take into account this aperture blockage. The illumination functions covered in the literature have not taken aperture blockage into consideration [8, 9]. The effect of gain reduction due to aperture blockage using illumination function correction is discussed in [12]. However, an illumination function taking into account the aperture blockage is not defined in [12]. Also, the far-field radiation pattern was not formulated in [12]. In this paper, a novel illumination function is defined that takes into account the aperture blockage created by the subreflector. Using this new illumination function, the AF integration is performed and a closed-form expression of the far-field radiation pattern is obtained. The derived expressions relate the aperture blockage to the radiation pattern directly. The obtained results are compared with the results obtained from the PO method and the PO + PTD methods, and are found to be consistent. The PO + PTD method uses a better approximation for the surface current density compared with the PO methods [1, 5]. This results in better accuracy. However, it is computationally more demanding compared to the PO method. As the PO and PO + PTD methods are generally accepted methods for far-field analysis of reflector antennas, the consistency of the derived results with the results obtained from these methods verifies the analysis.

The paper is organized as follows: Section II covers the geometry of the Cassegrain reflector, the illumination function is derived in Section III, Section IV contains the AF integration and far-field formulation, the numerical results are provided in Section V, and Section VI contains the concluding remarks.

II. GEOMETRY

The two-dimensional geometry of a Cassegrain antenna is shown in Fig 2. The following parameters are shown in Fig 2:

d_p = diameter of the main reflector,
d_s = diameter of the subreflector,

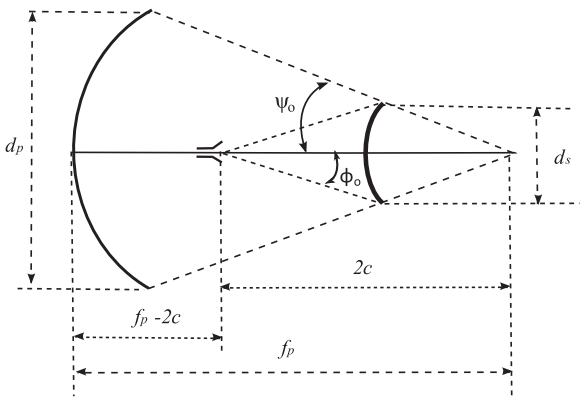

Fig. 2. Geometry of the Cassegrain reflector.

https://doi.org/10.1017/S1759078712000633 Published online by Cambridge University Press

f_p = focal length of the paraboloid,
$2c$ = distance between foci of the hyperboloid,
ψ_o = opening half angle of the paraboloid, and
ϕ_o = opening half angle of the hyperboloid.

The hyperboloidal subreflector has two focal points. One of the focal points coincides with the phase center of the feed horn and the other coincides with the focal point of the paraboloid [4]. The relation between the geometrical parameters can be found in [13].

To employ AF integration, it is necessary to project the main reflector surface on the aperture plane. For convenience, the aperture plane is assumed to go through the focal point of the main reflector [2, 4]. The angle ψ_o is created between the axis of the reflector and the line joining the focal point and edge of the main reflector. In general, angle ψ can be defined for any arbitrary point on the reflector surface. This angle varies from $-\psi_o$ to $+\psi_o$. The normalized radius of a main reflector surface point projected on the aperture plane, a, can be related to the geometrical parameters as [4]:

$$a = \frac{4f_p}{d_p}\tan\frac{\psi}{2}. \tag{1}$$

The variable a is depicted in Fig 1. It can be shown that [4]:

$$\tan\frac{\psi_o}{2} = \frac{d_p}{4f_p}. \tag{2}$$

From (1) and (2), it is clear that as the angle ψ varies from 0 to ψ_o, a varies from 0 to 1. Using (1), each point on the main reflector surface defined by an angle ψ can be mapped into the aperture plane defined by a normalized radius a.

III. DEFINING THE ILLUMINATION FUNCTION

The field distribution on the aperture plane is approximated by an illumination function. The phase distribution of the projected field on the aperture plane is often assumed to be constant [4, 8]. Well-designed feed horns can produce illumination with constant phase over the entire aperture, thus justifying the assumption. In such cases, the illumination function represents the variation in field amplitude over the aperture. The feed and therefore the resulting aperture distribution are usually circularly symmetric for an axially symmetric geometry. Thus, the illumination function can be expressed by the single independent variable a, and is denoted as $A(a)$.

The illumination function can be modeled as a Gaussian function, a raised-quadratic function, or other higher order polynomial functions [8, 9]. These functions represent a field distribution with maximum value near the bore-sight (axis of the reflector) and gradually taper at the edge. The ratio of the field value at the edge of the aperture to the maximum field value at the center of the aperture is known as the edge taper, T. Most illumination functions use the parameter T [8]. However, none of the illumination functions found in the literature take into account the decrease in the AF caused by the subreflector blockage.

In this paper, a new illumination function is defined as

$$A(a) = \begin{cases} g(a), & -a_e < a < a_e \\ f(a), & \text{otherwise} \end{cases} \tag{3}$$

Here, a_e is defined as the normalized radius of the aperture that is shadowed by the subreflector, $f(a)$ is the illumination function in the region where no aperture blockage has occurred, and $g(a)$ is the illumination function in the shadowed region describing the decreased AF caused by the subreflector blockage. The shadowed region is highlighted in Fig. 1.

Clearly, the parameter a_e is dependent on the subreflector diameter and the main reflector diameter. As $a = 1$ represents the radius of the main reflector ($d_p/2$) and a_e is related to the subreflector radius, it can be written intuitively that,

$$a_e = \frac{d_s/2}{d_p/2} = \frac{d_s}{d_p}. \tag{4}$$

The definition of $f(a)$ is taken from [8]:

$$f(a) = 1 - qga^2 + (q-1)ga^4. \tag{5}$$

where q is a parameter that is used to model a feed horn more accurately, and

$$g = 1 - T. \tag{6}$$

Here, T is the edge taper. As (5) contains even powers of a only, it is symmetric around the origin. The general shape of (5) is a function that has maximum value around the center region, and gradually decreases to T on both sides. This represents typical feed patterns. However, the overall illumination of the main reflector will have a different shape than this because of the subreflector blockage. It is expected that the subreflector will create a shadow around the axial region of the main reflector, causing a decrease in main reflector aperture illumination. This is modeled using the function $g(a)$ in the shadowed region ($-a_e < a < a_e$).

To keep a consistency with (5), the illumination function in the shadowed regions, $g(a)$, is also defined as a fourth-order polynomial:

$$g(a) = c + ma^2 + na^4. \tag{7}$$

Here, c, m, and n are parameters. The parameter c denotes the value of the illumination function at the center of the aperture where the blockage has maximum effect. Thus, c represents the maximum attenuation due to the subreflector blockage. The signs of these constants will be such that the function $g(a)$ will have a U-shaped nature. This implied that the $g(a)$ will have lowest value in the center of the main reflector where the blockage resulting shadowing is maximum. The value will gradually increase toward the edge of the shadowed region.

The parameters m and n can be related to other known parameters by enforcing continuity conditions. As the illumination function describes the AF distribution, it should be continuous and smooth. Hence, the two parts of $A(a)$ defined in (3) must be continuous and smooth at the edge transition point a_e. The following two equations are used to

https://doi.org/10.1017/S1759078712000633 Published online by Cambridge University Press

enforce these conditions:

$$f(a_e) = g(a_e). \tag{8}$$

$$\left.\frac{\mathrm{d}f(a)}{\mathrm{d}a}\right|_{a=a_e} = \left.\frac{\mathrm{d}g(a)}{\mathrm{d}a}\right|_{a=a_e}. \tag{9}$$

The continuity of the derivatives ensures that the transition is smooth.

Using (5) and (7) in (8):

$$ma_e^2 + na_e^4 = 1 - qga_e^2 + (q-1)ga_e^4 - c. \tag{10}$$

Calculating the derivatives from (5) and (7), and substituting them in (9):

$$m + 2na_e^2 = -qg + 2(q-1)ga_e^2. \tag{11}$$

The parameters m and n can be easily solved from (10) and (11) to yield the following results:

$$\left.\begin{aligned} m &= \frac{2(1-c)}{a_e^2} - qg \\ n &= (q-1)g - \frac{1-c}{a_e^4} \end{aligned}\right\}. \tag{12}$$

The parameter a_e can be calculated from the geometry using (4), the parameters q and g can be calculated from the feed horn characteristics, and the value of c can be approximated from the expected field reduction caused by the blockage. Thus, using (12), m and n can be calculated.

As all the parameters are defined and related to known quantities, the definition of the illumination function is complete. Figure 3 shows the plot of the defined illumination function for some arbitrary parameters. The q parameter does not significantly affect the shape of the illumination function. The value of $q = 0.4$ is used for numerical analysis in this paper.

IV. AF INTEGRATION AND FAR-FIELD FORMULATION

The far-field radiation pattern can be calculated by performing the AF integration [14]. An observation point $P(r, \theta, \varphi)$ in the far-field region is defined by its spherical coordinates (r, θ, φ). The point is shown in Fig. 1. For a circularly symmetric aperture distribution with constant phase, the far-field radiation pattern can be approximated by the following integral [4]:

$$f(\theta, \phi) = \frac{\pi d_p^2}{2} \int_{a=0}^{1} A(a) J_o\left(\frac{kd}{2} a \sin\theta\right) a \, \mathrm{d}a. \tag{13}$$

Here, $k = 2\pi/\lambda$=wave number, λ = wavelength and, $J_p(\cdot)$ = Bessel function of the first kind and order p. The angular coordinate variable, u is defined as:

$$u = \frac{kd}{2} \sin\theta. \tag{14}$$

Using (14) and substituting the value of the illumination function from (3) in (13), the integral becomes:

$$f(\theta, \phi) = \frac{\pi d_p^2}{2} \left[\int_{a=0}^{a_e} g(a) J_o(ua) a \, \mathrm{d}a + \int_{a=a_e}^{1} f(a) J_o(ua) a \, \mathrm{d}a \right]. \tag{15}$$

The value of $f(a)$ and $g(a)$ can be substituted from (5) and (7). The resulting formulation involves integrating product of polynomials and Bessel function. The necessary integration results are [15]:

$$\left.\begin{aligned} \int a J_o(ua)\,\mathrm{d}a &= \frac{a J_1(ua)}{u} \\ \int a^3 J_o(ua)\,\mathrm{d}a &= \frac{a^3 J_1(ua)}{u} - \frac{2a^2 J_2(ua)}{u^2} \\ \int a^5 J_o(ua)\,\mathrm{d}a &= \frac{a^5 J_1(ua)}{u} - \frac{4a^4 J_2(ua)}{u^2} + \frac{8a^3 J_3(ua)}{u^3} \end{aligned}\right\}. \tag{16}$$

To simplify the expressions, Bessel functions are replaced by Lambda function $\Lambda_p(.)$ defined as [15]:

$$\Lambda_p(u) = p! \frac{J_p(u)}{(u/2)^p}. \tag{17}$$

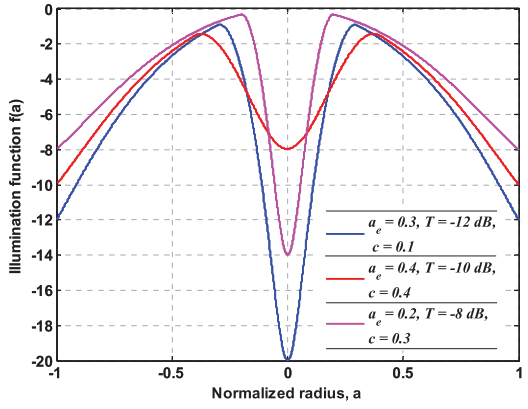

Fig. 3. Plot of the defined illumination function.

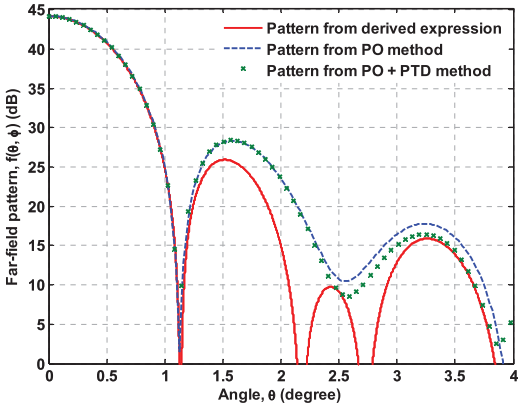

Fig. 4. Far-field radiation pattern.

https://doi.org/10.1017/S1759078712000633 Published online by Cambridge University Press

Table 1. Comparison of numerical results obtained from the derived method, PO method, and PO + PTD method.

Measured quantity	Derived method	PO method	Percentage error of derived method compared with PO method	Results from PO + PTD method	Percentage error of derived method compared with PO + PTD method
Gain (dB)	44.2	44.2	0	44.17	0.068
HPBW (degree)	0.944	0.944	0	0.942	0.2
First significant sidelobe level (dB)	25.93	28.33	8.47	28.4	8.69
Angular position of the first significant sidelobe (degree)	1.53	1.58	3.16	1.56	1.92
Second significant sidelobe level (dB)	15.89	17.77	10.58	16.44	3.35
Angular position of the second significant sidelobe (degree)	3.26	3.24	0.62	3.25	0.31

After evaluating the integrals in (15) and normalizing the results, the obtained expression of normalized far-field radiation pattern, $f_N(\theta, \phi)$ is:

$$f_N(\theta,\phi)=\frac{1}{N}\left[\Lambda_1(u)\left(\frac{1-g}{2}\right)+\Lambda_2(u)g\left(\frac{2-q}{4}\right)+\Lambda_3(u)g\left(\frac{q-1}{6}\right)+\Lambda_2(ua_e)\left\{\frac{qga_e^4\left(1-a_e^3\right)}{4}\right\}+\Lambda_3(ua_e)\left\{\frac{a_e^2(1-c)}{6}\right\}\right]. \quad (18)$$

Here, the normalizing factor, N is given by:

$$N=\frac{1}{12}\left\{6-2g-2a_e^2(1-b)+qg\left(3a_e^4-3a_e^7-1\right)\right\}. \quad (19)$$

Equation (18) gives the approximate closed-form expression of the far-field radiation pattern of the Cassegrain antenna, which is expected to be sufficiently accurate near the main-lobe region of the antenna.

V. NUMERICAL RESULTS

For numerical analysis, a standard Cassegrain antenna with the main reflector diameter $d_p = 2$ m, primary focal length $f_p = 0.8$ m, subreflector diameter $d_s = 0.5029$ m, and distance between subreflector foci $2c = 0.7$ m is assumed. The relation between these parameters and other geometrical parameters are calculated using the method described in [13]. A typical edge taper of 10 dB is assumed, implying $T = 10^{-10/20} = 0.3162$. The parameter a_e is found from (4) as 0.25145. The operating frequency is assumed to be 10 GHz. It is found that for the defined geometry and edge taper, $q = 0.4$ accurately describes a conical corrugated horn feed. The q parameter value is calculated using the method described in [8].

The far-field radiation pattern calculated using (18) and using the standard PO method [5] is shown in Fig. 4. It can be seen from Fig 4 that the main-lobe patterns obtained from the two methods are exactly the same. The first few sidelobe levels obtained from the derived expression differ from the results of the PO method only by a few dB. The results are summarized in Table 1. It can be observed from the data that the gain and half-power beamwidth (HPBW) computed from the derived method are almost identical to the results obtained from the PO and PO + PTD methods, showing a maximum error of only 0.2% (accuracy of 99.8%). The proposed method has an error around 2–3% in identifying the angular position of the first sidelobe. The error in computing the first sidelobe level is around 8–9%. This implies that the prediction of the first sidelobe is up to 91% accurate. The proposed method also satisfactorily predicts the position and the amplitude level of the second significant level with errors as little as 0.3% and 3.35%, respectively, when compared with the PO + PTD method. This error is higher when compared with the PO method (without PTD correction). However, PO + PTD methods are expected to have more accuracy in sidelobe regions compared with the PO method. Thus, the derived equations also have excellent agreement in the second sidelobe region as well.

For a simplified closed-form expression, the accuracy of the derived equations can be considered satisfactory. The closed-form expression can be used for approximating the main-lobe and the first few sidelobes for cases where quick calculations are required. The PO method and PO + PTD method are computationally demanding and require significant simulation time for large reflectors [5]. As the derived expression is closed form, the simulation time is drastically reduced.

VI. CONCLUSION

An illumination function for estimating the AF distribution is defined. The function takes into account the effect of subreflector blockage. Using the illumination function, the far-field radiation pattern is estimated by performing AF integration. A closed-form expression is obtained from the integration. The obtained results are compared with results from the PO method and the PO + PTD method, which are universally accepted as valid methods for reflector analysis. It is found that the results are in excellent agreement in the main-lobe region. As the radiation pattern of only the main-lobe region is often required, the derived method provides sufficient accuracy. Also, simulation time for the proposed method is much smaller compared with the PO method as the obtained results are closed-form.

REFERENCES

[1] Rahmat-Samii, Y.: In Reflector Antennas, Volakis, J.L. (Ed.), Antenna Engineering Handbook, chapter 15, 4th ed., McGraw-Hill, USA, 2007.

https://doi.org/10.1017/S1759078712000633 Published online by Cambridge University Press

[2] Balanis, C.A.: Antenna Theory Analysis and Design, 3rd ed., John Wiley & Sons, New Jersey, USA, 2005.

[3] Silver, S.: Microwave Antenna Theory and Design, McGraw-Hill, New York, USA, 1949.

[4] Baars, J.W.M.: The Paraboloidal Antenna in Radio Astronomy and Communication, Springer, New York, USA, 2007.

[5] McNamara, D.A.; Pistorius, C.W.I.; Malherbe, J.A.G.: Introduction to the Uniform Geometrical Theory of Diffraction, Artech House, Norwood, MA 02062, USA, 1990.

[6] Yaghjian, A.: Equivalence of surface current and aperture field integrations for reflector antennas. IEEE Trans. Antennas Propag., **32** (1984), 1355–1358.

[7] Bucci, O.; Franceschetti, G.; Pierri, R.: Reflector antenna fields – an exact aperture-like approach. IEEE Trans. Antennas Propag., **29** (1981), 580–586.

[8] Zaman, M.A.; Choudhury, S.M.; Gaffar, M.; Matin, M.A.: Modeling the illumination function of a Cassegrain reflector for a corrugated horn feed and calculation of the far field pattern, in Proc. Loughborough Antennas & Propagation Conf., November 2009, 101–104.

[9] Richardson, R.J.: A new family of illumination functions. IEEE Trans. Antennas Propag., **18** (1970), 284–285.

[10] Pace, J.R.: Aperture blockage by a subreflector in a Cassegrain antenna system. Electron. Lett., **4** (1968), 500–501.

[11] Lamb, J.W.; Oliver, A.D.: Blockage due to subreflector supports in large radiotelescope antennas. Proc. IEE Microw. Antennas Propag., **133** (1986), 43–49.

[12] Solovey, A.; Cardiasmenos, A.; Mittra, R.: An optical blockage illumination correction factor for circular reflectors, in Proc. IEEE Antennas and Propagation Society Int. Symp., June 2007, 5155–5158.

[13] Granet, C.: Designing axially symmetric Cassegrain or Gregorian dual-reflector antenna from combinations of prescribed geometric parameters. IEEE Antennas Propag. Mag., **40** (1998), 76–82.

[14] Munro, E.W.; Whitaker, A.J.T.; McInnes, P.A.: Calculations of the secondary radiation pattern for a paraboloid reflector with a given illumination function and feed position. Electron. Lett., **9** (1973), 234–235.

[15] Polyanin, A.D.; Manzhirov, A.V.: Handbook of Mathematics for Engineers and Scientists, Chapman & Hall/CRC, New York, USA, 2007.

https://doi.org/10.1017/S1759078712000633 Published online by Cambridge University Press